Supplementary Information

Micro-crumpled composite film electrodes based flexible capacitive sensor with broad sensing range for human physiological signal and gesture monitoring

Qiang Zhao, [a, b] Lei Fan, [a, b] Nan Zhao, [c] Haoyun He, [a, b] Lei Zhang*[a, b] and Qiulin Tan*[a, b]

[a] Key Laboratory of Instrumentation Science & Dynamic Measurement, Ministry of Education, North University of China, Tai Yuan 030051, China;

[b] Science and Technology on Electronic Test and Measurement Laboratory, North University of China, Tai Yuan 030051, China;

[c] National Key Laboratory of Science and Technology on Micro/Nano Fabrication, Shanghai Jiao Tong University, Shanghai 200240, China

* Correspondence: tanqiulin@nuc.edu.cn; Tel.: +86-351-3557-328

Table of Contents

Supplementary Text

Sample preparation and characterization for TEM:

Samples for TEM of the $Ti_3C_2T_x$ MXene nanosheets were prepared by the drop-casting method. The $Ti_3C_2T_x$ MXene dispersion was first diluted down to 0.01 mg/ml. A portion of the dispersion was then collected in a dropper and carefully drop-coated onto lacey carbon films supported on a Cu grid. After the grid was dried in air, it was placed on the front end of the sample rod, and subsequently the sample rod carrying the grid was placed into the TEM image chamber, which was examined using a transmission electron microscope when the vacuum of the image chamber reached the required level and was equipped with a probe to form an aberration correction of the lens. To improve the spatial resolution, all TEM images were acquired at an acceleration voltage of 200 kV.

Sample preparation and characterization for XPS:

$Ti_3C_2T_x$ MXene samples for XPS testing were prepared through vacuum filtration of the MXene dispersion, followed by drying of the films using a vacuum drying oven. The film samples were cut into square pieces (5 mm × 5 mm) and affixed to a sample test bench for testing. Samples were analyzed using the XPS system (ESCALAB 250 Xi, UK) with a monochromatic Al Kα X-ray beam (1486.6 eV). The XPS patterns were obtained with the following parameters: Spot size: 500 μm; Lens Mode: standard electrostatic; Analyser Mode: constant analyzer energy; Pass Energy:20 eV; Energy Step Size: 0.05 eV; Number of Energy Steps: 801; Number of Scans: 10. The binding energies of the spectra in the XPS results were calibrated by using C 1s (284.6 eV) as a reference.

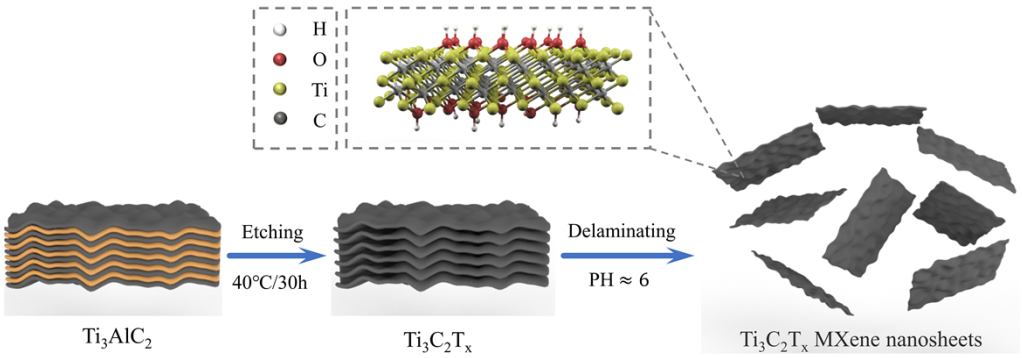

Fig.S1. The fabrication process of $Ti_3C_2T_x$ MXene nanosheets.

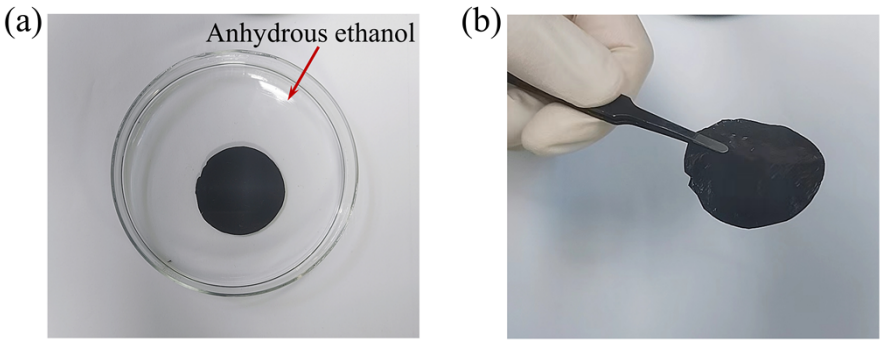

Fig.S2. The digital photographs of the flexible and freestanding S-MXene composite film.

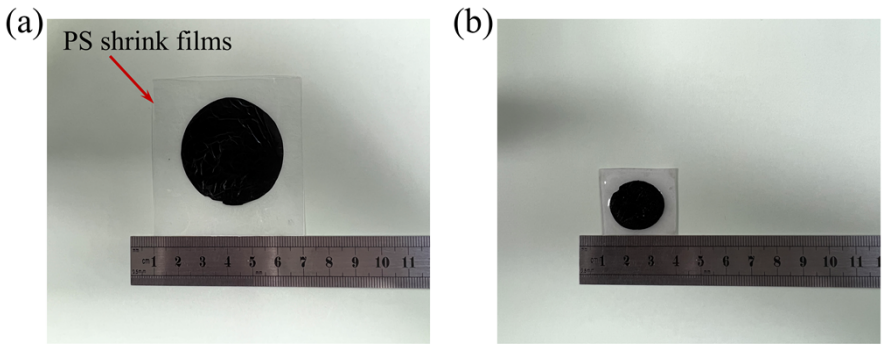

Fig.S3. Comparison of S-MXene composite films (a) before thermal shrinkage, (b) after thermal shrinkage.

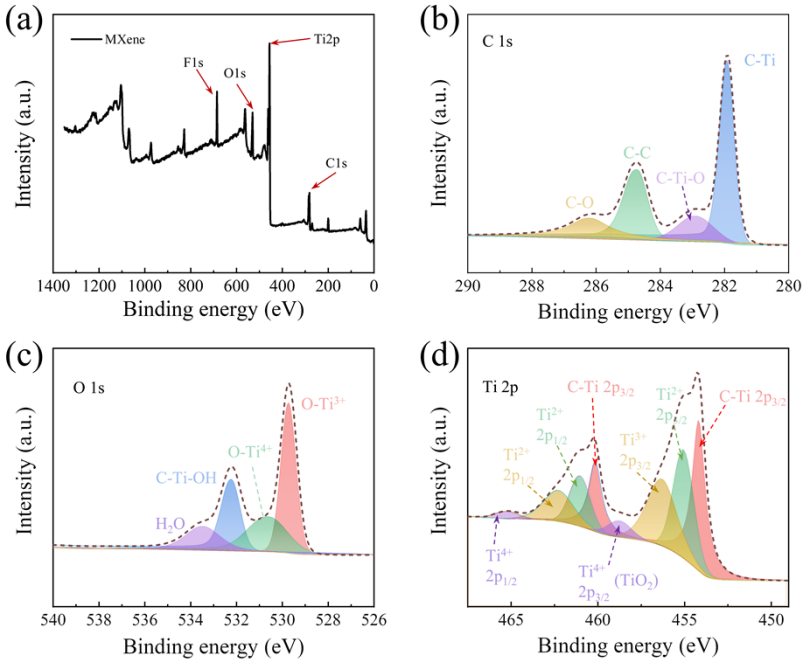

Fig.S4. XPS spectra characterization of $Ti_3C_2T_x$ MXene film. (a) XPS spectra of $Ti_3C_2T_x$ MXene. High-resolution XPS spectra of (b) C 1s, (c) O 1s and (d) Ti 2p of $Ti_3C_2T_x$ MXene. The full spectrum images of $Ti_3C_2T_x$ MXene confirm the existence of Ti, C, O and F elements, the contents of Ti, C, O, F elements are 46.76%, 25.91%, 19.52%, and 7.81%, respectively. The C 1s spectra of $Ti_3C_2T_x$ MXene can be fitted into four peaks at 281.91 eV, 282.89 eV, 284.70 eV and 286.17 eV, which correspond to Ti-C, C-Ti-O, C-C and C-O bonds, respectively. The C 1s peak at 284.54 eV is carbon contamination caused by hydrocarbons adsorbed on instrument surface. Ti-C is the dominant chemical bond in $Ti_3C_2T_x$ MXene. Additionally, the C-Ti-O bond is formed by -OH adsorbed on the surface of $Ti_3C_2T_x$[1]. O 1s spectra of $Ti_3C_2T_x$ MXene can be fitted into four peaks at 529.70 eV, 530.59 eV, 532.21 eV and 533.44 eV, respectively, belonging to O-Ti^{3+}, O-Ti^{4+}, C-Ti-OH and H_2O. The Ti 2p orbital of $Ti_3C_2T_x$ MXene can also be fitted into four groups of the double peaks: Ti $2p_{3/2}$ peak and Ti $2p_{1/2}$ peak. The binding energies of Ti $2p_{3/2}$ peak at 454.15eV, 455.02 eV, 456.27 eV and 458.72 eV are attributed to Ti-C, Ti^{2+}, Ti^{3+} and Ti^{4+}(TiO_2), respectively. The binding energies of Ti $2p_{1/2}$ peak at 460.15 eV, 461.02eV, 462. 27eV and 465.23eV are attributed to Ti-C, Ti^{2+}, Ti^{3+} and Ti^{4+}(TiO_2), respectively.

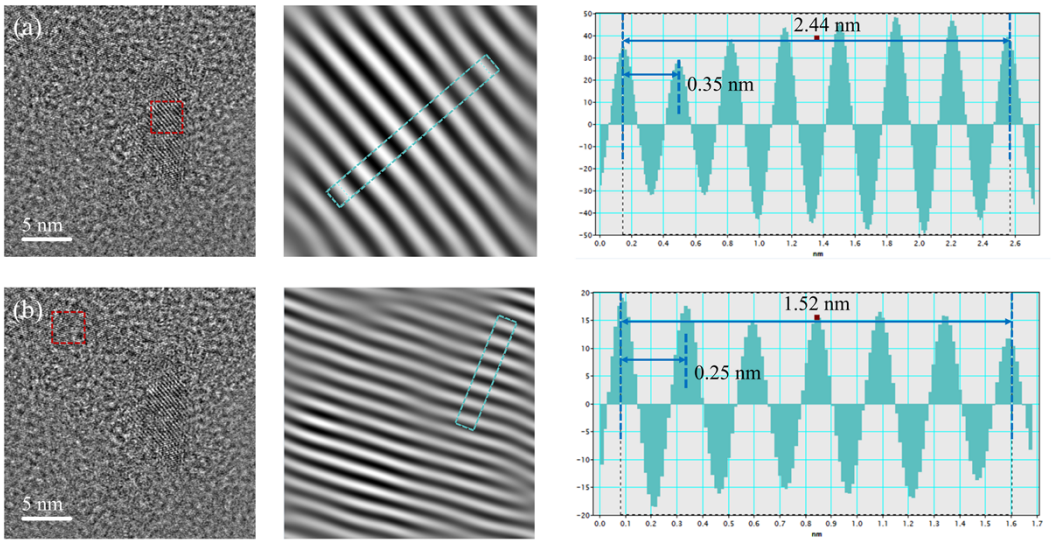

Fig.S5. HR-TEM of $Ti_3C_2T_x$ nanosheets and their corresponding line profiles of selected parts in panel (a) and panel (b).

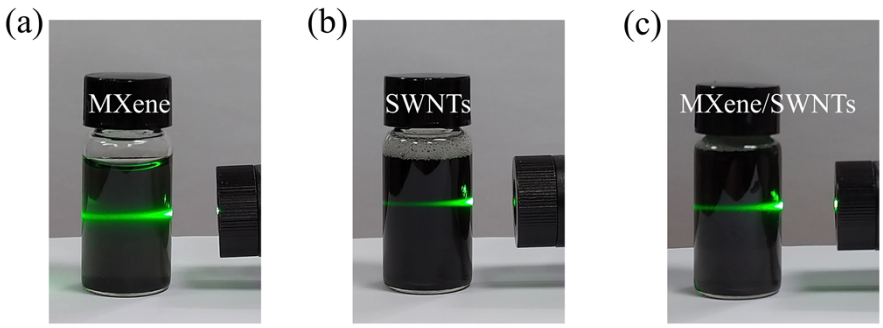

Fig.S6. The digital photographs of (a) MXene, (b) SWNTs and (c) MXene/SWNTs dispersions. From the illustrated diagram, both the MXene dispersion, SWNTs dispersion, and the MXene/SWNTs blend dispersion exhibit the Tyndall effect under light stimulation, indicating their effective dispersion.

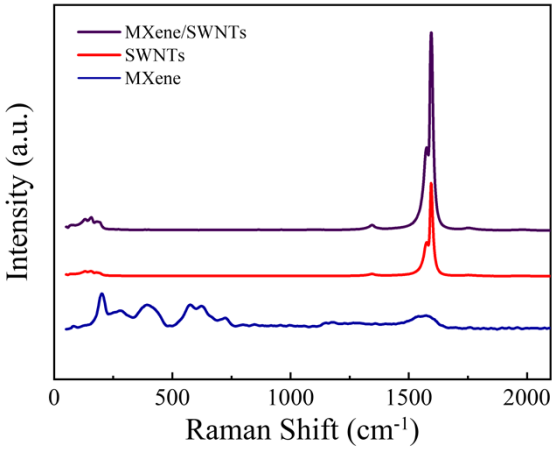

Fig.S7. Raman spectra of MXene film, SWNTs film, and S-MXene composite film.

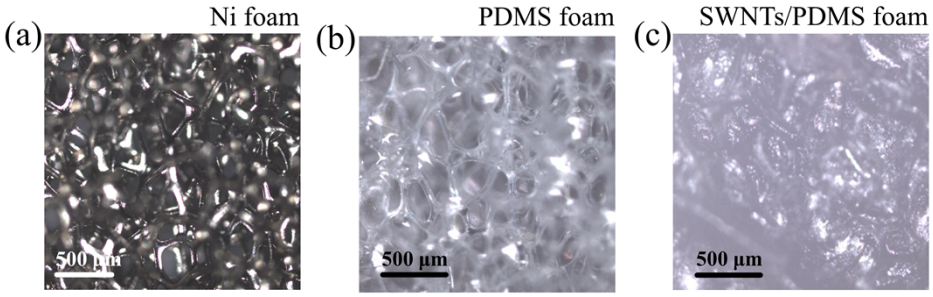

Fig.S8. Optical electron microscopy of (a) nickel foam and (b) PDMS foam (0 wt% SWNTs) and (c) S-PDMS foam (1.2 wt% SWNTs). As depicted in Figure (b), it is evident that a highly porous PDMS foam is prepared after the completion of etching.

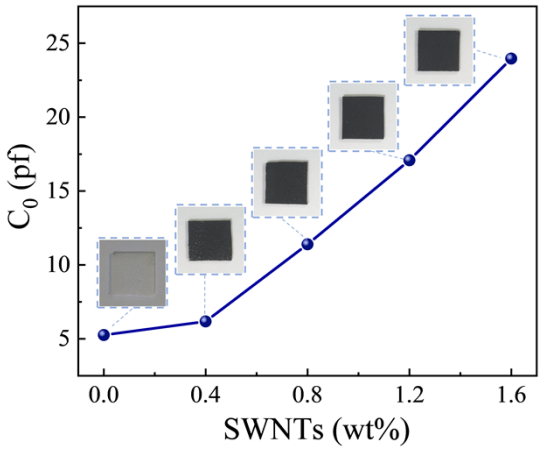

Fig.S9. The initial capacitance (C_0) of the pressure sensor with different SWNTs doping content (0, 0.4, 0.8, 1.2, and 1.6 wt%) at 10kHz frequency and room temperature. The inset shows the PDMS foam dielectric layers with different SWNTs doping content.

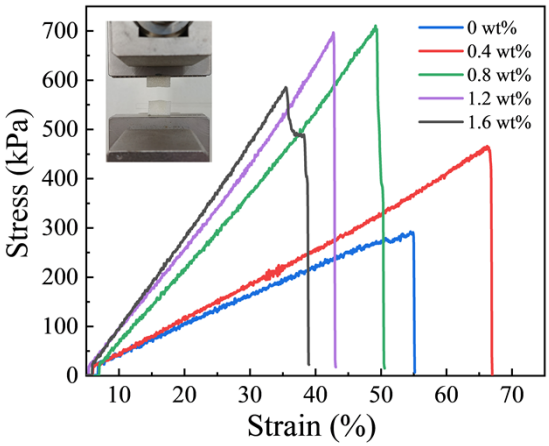

Fig.S10. Stress-strain curve of PDMS forms with different SWNTs

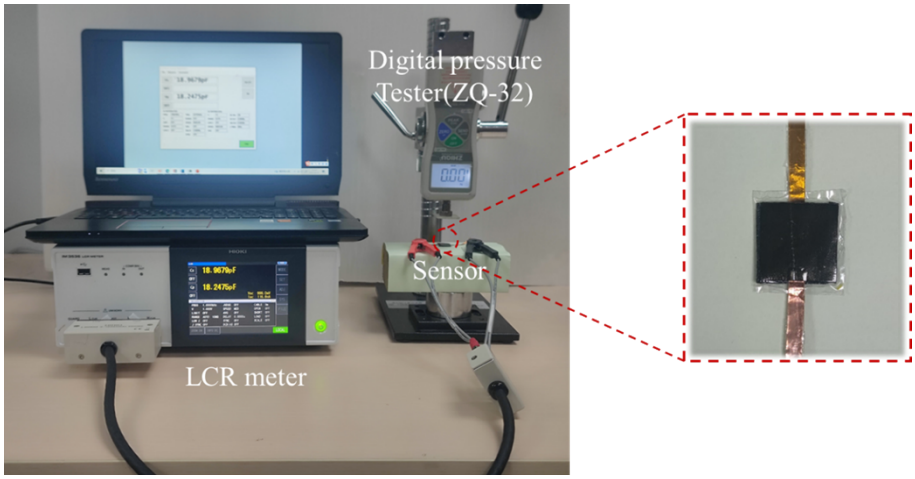

Fig.S11. Experimental setup for sensor response time testing.

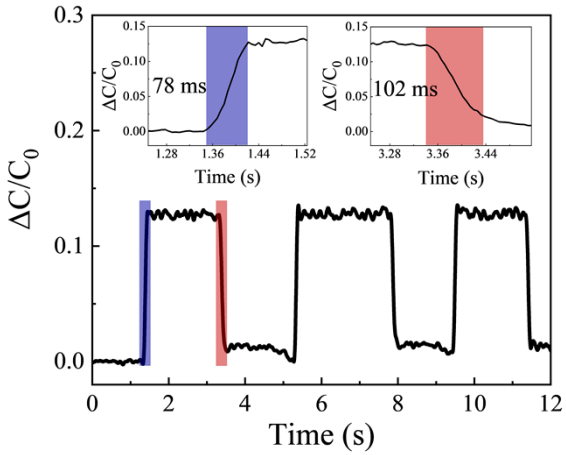

Fig.S12. The response and recovery times of flexible CPS using planar S-MXene composite films as electrodes.

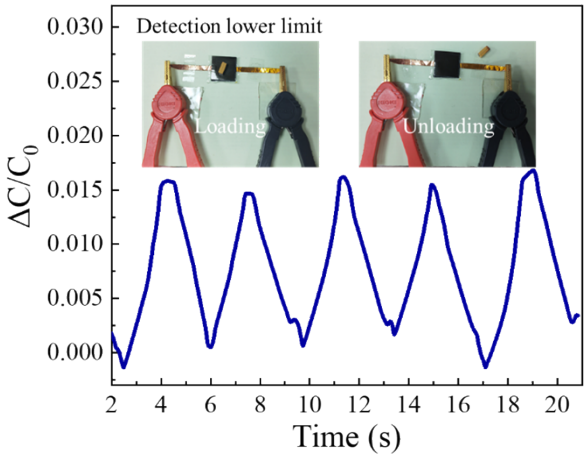

Fig.S13. Detection limit test of the SMCPS.

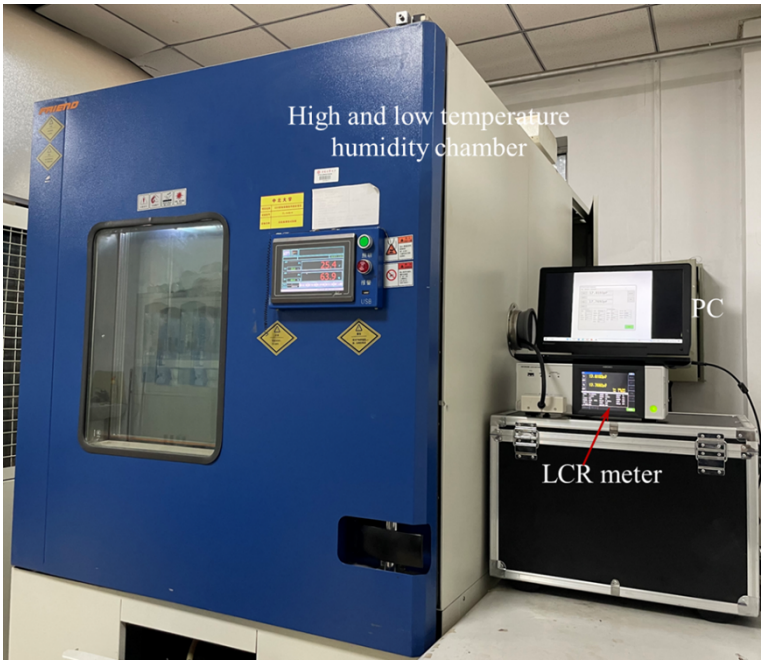

Fig.S14. The temperature and humidity resistance test platform.

The detailed information of the optimized smart gloves is presented below. To account for variations in finger dimensions among individuals, different-sized SMCPSs were prepared and attached to their corresponding finger positions. This ensures a more distinct and accurate signal output from the SMCPS at each finger site. Three sizes of SMCPSs were prepared, as illustrated in Fig.S15(a).

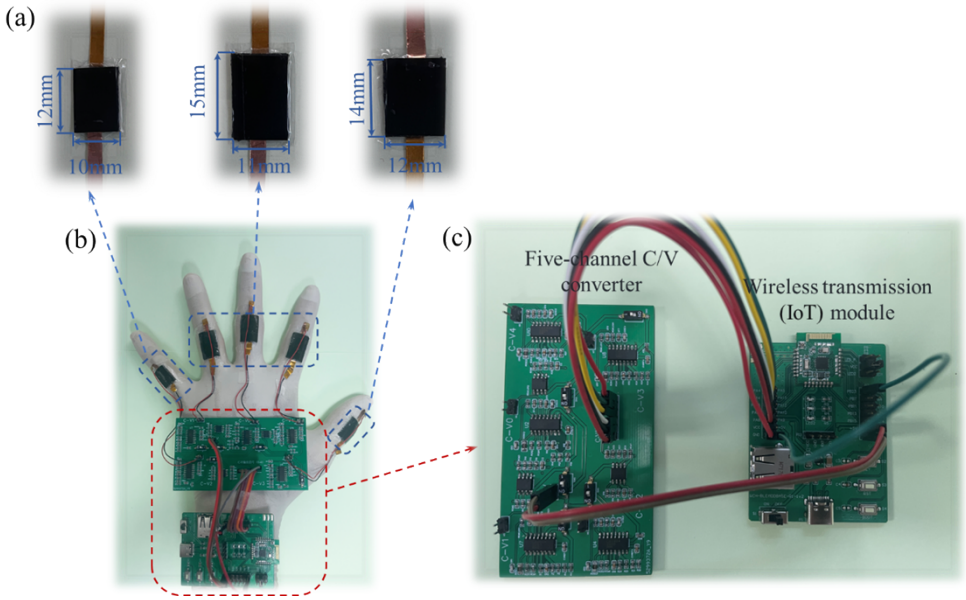

Fig.S15. Diagram illustrating the details of smart gloves. (a) The SMCPSs in three different sizes. (b) Schematic representation of the smart glove. (c) Signal acquisition circuitry and IoT module for wireless communication.

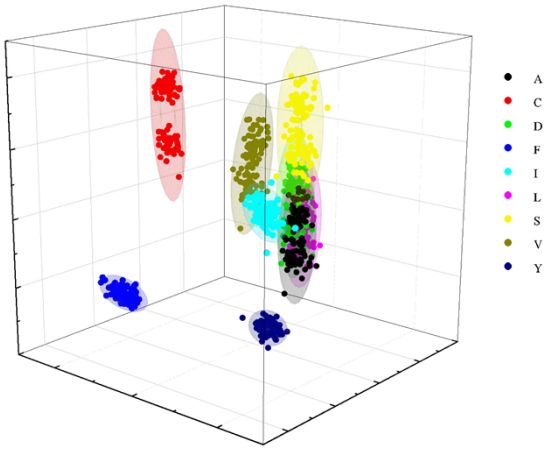

Fig.S16. The PCA clustered results for 9 gestures.

References and Notes

1 C. Peng, X. Yang, Y. Li, H. Yu, H. Wang and F. Peng, *ACS Appl Mater Interfaces*, 2016, **8**, 6051–6060.